solvent activation, a sulfiding agent with a high sulfur content, and a high-oxidation-state metalate precursor if it is to produce highly crystalline NiS_2. Extension of this type of precursor synthesis to other transition-metal chalcogenides should be possible. Sodium sulfides were chosen as the sulfiding agents because of their wide range of stoichiometries (Na_2S_y, $y = 1, 2, 4,$ and 5) and the high solubility of the sodium salt byproducts in water, but other alkali-metal sulfides could be used in place of sodium sulfide. In addition, alkali-metal selenides and alkali-metal tellurides can be prepared and should act as precursors to form transition-metal selenides and transition-metal tellurides. Other possible metal-containing precursors include binary halides in which the transition metal or main-group metal is stabilized in a high oxidation state. We are currently exploring precursor reactions involving the latter reagents.

Conclusions

A rapid low-temperature solid-state synthesis of crystalline nickel disulfide has been developed. The best precursors found are K_2NiF_6 and $Na_2S_5 \cdot 0.06H_2O$. They react at ~65 °C in seconds to produce pure, crystalline nickel disulfide. The KF, NaF, and S byproducts can be easily removed by washing. The crystallinity of the nickel disulfide from the precursor reaction is comparable to the crystallinity of nickel disulfide prepared at 450–500 °C over several days from nickel monosulfide and sulfur or from the elements. Increasing the amount of water used in the precursor reaction or lowering the oxidation state of the transition metal results in lower crystallinity for the NiS_2 product. Lowering the sulfur content of the sodium sulfide reagent from Na_2S_5 to Na_2S_2 or Na_2S leads to mixtures of nickel monosulfide and nickel disulfide.

Acknowledgment. This work was supported by the National Science Foundation, Grant No. CHE 8657822, through the Presidential Young Investigator Award Program along with matching funds provided by the ARCO Foundation.

Contribution from the Chemistry Departments, California State University, Sacramento, California 95819, and University of Hull, Hull HU6 7RX, U.K.

The First Second-Row Triketone Complex Structure: Synthesis and Properties of a Substituted (1,3,5-Pentanetrionato)(μ-oxo)bis(dioxomolybdenum(VI))

Londa L. Borer*[1a] and Ekkehard Sinn*[1b]

Received June 23, 1989

Reaction of the β-triketone ligand 1,5-diphenyl-1,3,5-pentanetrione with molybdenum(VI) produces the first such derivatives with a second-row transition-metal element. The products are oxygen-bridged binuclear complexes, with structural resemblance to olefin epoxidation catalysts. When synthesized from ethanol solution, the product contains one molecule of ethanol per molecule of binuclear complex and is highly insoluble, suggesting a polymeric structure. When recrystallized from dimethyl sulfoxide, the product is a crystalline (1,3,5-pentanetrionato)(μ-oxo)bis((dimethyl sulfoxide)dioxomolybdenum(VI)) complex, shown by X-ray crystallography to have a coordinated DMSO on each molybdenum to make up a six-coordinated environment: Crystal data for $(MoO_2)_2(C_{17}H_{12}O_3)(O)(DMSO)_2$: space group $P2_1/n$ with $Z = 4$, $a = 8.093$ (3) Å, $b = 22.724$ (6) Å, $c = 14.087$ (6) Å, $\beta = 90.21$ (3)°; the structure was refined to an $R(F_o^2)$ value of 4.9% for 2240 reflections.

Introduction

Interest in the β-polyketonate ligand systems stems from their ability to chelate two or more metal ions with the resultant formation of four-membered rings containing two metal atoms and two bridging oxygens. The complexes of the simpler 1,3-diketones have been well characterized, and recently chelates of 1,3,5-triketonates have received considerable attention. Several key papers have dealt with the structure, magnetism, and electrochemistry of Cu(II),[2] Ni(II),[3] Co(II),[4,5] Fe(III),[6] Cr(III),[7] and $V^{II}O$,[8] all first-row transition metals. Higher homologue chelates containing UO_2 have also been reported,[9] as have complexes of the hexadentate ligand generated by condensation of two triketones with diamines.[10] Mo(VI) complexes are of interest because these are known to catalyze such reactions as the epoxidation of olefins and the oxidations of alcohols.[11-13]

Table I. Crystal Data for a (1,3,5-Pentanetrionato)(μ-oxo)bis(dimethyl sulfoxide)dioxomolybdenum(VI) Complex, $(MoO_2)_2(C_{17}H_{12}O_3)(O)(DMSO)_2$

$Mo_2S_2O_{10}C_{21}H_{24}$
fw = 692
$a = 8.093$ (3) Å
$b = 22.724$ (6) Å
$c = 14.087$ (6) Å
$\beta = 90.21$ (3)°
$V = 2591$ (3) Å^3
$Z = 4$

space group: $P2_1/n$ (No. 14)
$T = 23$ °C
$\lambda(\text{Mo K}\alpha) = 0.71069$ Å
$\rho_{calc} = 1.78$ g/cm^3; $\rho_{obs} = 1.74$ g/cm^3
$\mu(\text{Mo K}\alpha) = 11.6$ cm^{-1}
transm coeff = 0.91, 0.86
$R(F_o^2) = 0.049$
$R_w(F_o^2) = 0.062$

---

(1) (a) California State University. (b) University of Hull.

(2) (a) Fenton, D. E.; Schroeder, R. R.; Lintvedt, R. L. *J. Am. Chem. Soc.* **1978**, *100*, 6. (b) Lintvedt, R. L.; Kramer, L. S. *Inorg. Chem.* **1983**, *22*, 796. (c) Lintvedt, R. L.; Ranger, G.; Schoenfelner, B. A. *Inorg. Chem.* **1984**, *23*, 688.

(3) Lintvedt, R. L.; Ranger, G.; Ceccarelli, C. *Inorg. Chem.* **1985**, *24*, 2359.

(4) Glick, M. D.; Lintvedt, R. L. *Prog. Inorg. Chem.* **1978**, *21*, 233 and references cited therein.

(5) Lintvedt, R. L.; Tomlonovic, B. K.; Fenton, D. E.; Glick, M. D. *Adv. Chem. Ser.* **1976**, *No. 50*, 407.

(6) Borer, L. L.; Vanderbout, W. *Inorg. Chem.* **1979**, *18*, 526.

(7) Borer, L. L.; Horsma, R.; Rajan, O. A.; Sinn, E. *Inorg. Chem.* **1986**, *25*, 3652.

(8) Lintvedt, R. L.; Glick, M. D.; Tomlonovic, B. K.; Gavel, D. P. *Inorg. Chem.* **1976**, *15*, 1646.

(9) Lintvedt, R. L.; Schoenfelner, B. A.; Ceccarelli, C.; Glick, M. D. *Inorg. Chem.* **1984**, *23*, 2867.

(10) (a) Ahmad, N. *Inorg. Chim. Acta* **1989**, *155*, 237. (b) Casellato, U.; Vigato, P. A.; Fenton, D. E.; Vidali, M. *Chem. Soc. Rev.* **1979**, *8*, 199. (c) Fenton, D. E.; Gayda, S. E. *J. Chem. Soc., Dalton Trans.* **1977**, 2095, 2102, 2109. (d) Vigato, P. A.; Casellato, U.; Tamburini, S.; Milani, F.; Musiani, M. M. *Inorg. Chim. Acta* **1982**, *61*, 89.

(11) Bortolini, O.; Conte, V.; DiFuria, F. D.; Modena, G. *Nouv. J. Chim.* **1985**, *9*, 147.

(12) Sheldon, R. H.; van Doorn, J. A. *J. Catal.* **1973**, *31*, 427.

(13) Bortolini, O.; DiFuria, F.; Modena, G. *J. Mol. Catal.* **1982**, *14*, 53.

0020-1669/90/1329-2514$02.50/0 © 1990 American Chemical Society

As part of a general study of binuclear metal complexes of the β-polyketonate ligand system, we have synthesized and investigated the properties of two molybdenum(VI) complexes of 1,5-diphenyl-1,3,5-pentanetrione. Prior to this report on a (1,5-diphenyl-1,3,5-pentanetrionato)(μ-oxo)dimolybdenum(VI)–bis(dimethyl sulfoxide), no single-crystal X-ray structure on a second-row transition-metal triketonate has been reported. This complex and Pd(II) derivatives[14] constitute the only reported complexes of such ligands with second-row metals.

Experimental Section

Synthesis of $(MoO_2)_2(C_{17}H_{12}O_3)(O)(C_2H_5OH)$ and $(MoO_2)_2(C_{17}H_{12}O_3)(O)(DMSO)_2$. A 0.332-g (1.25-mmol) sample of 1,5-diphenyl-1,3,5-pentanetrione, prepared by the method of Hauser et al.,[15] was dissolved in ethanol (50 mL). The solution was heated to reflux and 1.117 g (3.42 mmol) of $MoO_2(acac)_2$[16] in ethanol (30 mL) was added slowly. The resultant solution was refluxed for 1 h. A brown solid precipitated when the volume of solution was reduced. The precipitate was collected, washed with ethanol and methylene chloride, and dried in vacuo. Anal. Found: C, 39.38; H, 2.73; Mo, 33.33. Calcd for $C_{19}H_{18}O_9Mo_2$: C, 39.17; H, 3.09; Mo, 32.99. Yellow crystals of $(MoO_2)_2(C_{17}H_{12}O_3)(O)(DMSO)_2$ suitable for single-crystal X-ray diffraction study were prepared by heating the brown solid to boiling in DMSO for 1 h and then allowing the solution to cool and stand at room temperature. The crystals separated from the solution after several days.

Physical Measurements. Infrared spectra were measured on potassium bromide disks by using a Perkin-Elmer FTIR instrument.

UV and visible spectra were measured for 1×10^{-4} M solutions on a Perkin-Elmer Diode Lambda Array spectrophotometer.

Proton NMR spectra were measured on a Varian FT-80A instrument in DMSO-d_6 solution.

Cyclic voltammograms were obtained on a BAS-100 electrochemical analyzer by using 2×10^{-3} M DMSO solutions with tetraethylammonium perchlorate as supporting electrolyte (0.1 M).

Magnetic susceptibilities in the 10–277 K temperature range were determined on a SHE SQUID magnetometer. Calibration and operation of this instrument are described elsewhere.[17,18]

Crystal Data and Data Collection (Table I). The crystal chosen for data collection had dimensions as follows (mm from centroid): (100) 0.23, $(\bar{1}00)$ 0.23, (010) 0.14, $(0\bar{1}0)$, 0.14, (001) 0.09, $(00\bar{1})$ 0.09. Cell dimensions and space group data for the molecule were obtained by standard methods on an Enraf-Nonius four-circle CAD4 diffractometer. The θ–2θ scan technique was used as previously described,[19] to record the intensities for all nonequivalent reflections for which $1° < 2\theta < 50°$. Scan widths were calculated as $(A + B \tan \theta)°$, where A is estimated from the mosaicity of the crystal and B allows for the increase in width of peak due to $K\alpha_1$–$K\alpha_2$ splitting. The values of A and B were 0.62° and 0.35°, respectively.

The intensities of three standard reflections showed no greater fluctuations than those expected from Poisson statistics. The raw intensity data was corrected for Lorentz-polarization effects and absorption. Of the 4853 independent intensities, there were 2240 with $F_o^2 \geq 3.00\sigma(F_o^2)$, where $\sigma(F_o^2)$ was estimated from counting statistics.[20]

Structure Determination. The positions of the metal and sulfur atoms were determined from three-dimensional Patterson functions. The intensity data was phased sufficiently well by these positional coordinates to permit location of the other non-hydrogen atoms from Fourier difference syntheses. Full-matrix least-squares refinement was carried out by using the TEXRAY program set. When anisotropic temperature factors were introduced, further Fourier difference syntheses permitted location of the hydrogen atoms, which were included in the refinement for two cycles and then held fixed. The model converged with $R(F_o^2) = 4.9\%$ and $R_w(F_o^2) = 6.2\%$. Final Fourier difference functions showed no peaks higher than 0.93 e/Å^3. Tables of the observed and calculated structure factor are available,[21] together with least-squares planes and extended bond angle calculations.

Table II. Positional Parameters for $(MoO_2)_2O(PhTriket)(DMSO)_2$

atom	x	y	z
Mo1	0.4137 (1)	0.20571 (4)	0.05180 (7)
Mo2	0.5218 (1)	0.14024 (4)	0.24936 (7)
S1	0.8122 (4)	0.1772 (1)	0.0295 (2)
S2	0.1009 (4)	0.1542 (1)	0.2608 (2)
O1b	0.528 (1)	0.2086 (3)	0.1693 (5)
O1s	0.640 (1)	0.1575 (3)	−0.0008 (6)
O2s	0.274 (1)	0.1744 (3)	0.2888 (5)
O2b	0.3808 (9)	0.1178 (3)	0.1171 (5)
O11	0.333 (1)	0.1599 (3)	−0.0613 (5)
O12	0.221 (1)	0.2243 (3)	0.0853 (5)
O13	0.484 (1)	0.2679 (3)	−0.0011 (5)
O21	0.407 (1)	0.0654 (3)	0.2867 (5)
O22	0.590 (1)	0.1657 (3)	0.3546 (5)
O23	0.691 (1)	0.1041 (3)	0.2073 (6)
C1	0.257 (1)	0.0949 (5)	−0.1817 (8)
C1s	0.931 (2)	0.1123 (6)	0.022 (1)
C2	0.229 (2)	0.1433 (6)	−0.2393 (9)
C2s	0.898 (2)	0.2164 (7)	−0.067 (1)
C3	0.180 (2)	0.1356 (8)	−0.333 (1)
C3s	−0.021 (2)	0.2194 (6)	0.267 (1)
C4	0.154 (2)	0.0799 (8)	−0.367 (1)
C4s	0.027 (2)	0.1191 (5)	0.362 (1)
C5	0.185 (2)	0.0319 (6)	−0.313 (1)
C6	0.235 (2)	0.0399 (5)	−0.218 (1)
C7	0.310 (1)	0.1045 (5)	−0.0825 (8)
C8	0.322 (1)	0.0596 (5)	−0.0174 (8)
C9	0.360 (1)	0.0658 (5)	0.0801 (7)
C10	0.354 (2)	0.0160 (5)	0.1430 (8)
C11	0.367 (1)	0.0173 (5)	0.2393 (8)
C12	0.346 (2)	−0.0346 (5)	0.2992 (8)
C13	0.360 (2)	−0.0284 (5)	0.3963 (9)
C14	0.342 (2)	−0.0767 (7)	0.458 (1)
C15	0.304 (2)	−0.1305 (6)	0.418 (1)
C16	0.286 (2)	−0.1385 (6)	0.323 (1)
C17	0.305 (2)	−0.0892 (6)	0.2639 (9)
H1s1	0.891	0.081	0.060
H1s2	0.933	0.097	−0.044
H1s3	1.047	0.119	0.038
H2	0.213	0.185	−0.217
H2s1	1.005	0.235	−0.051
H2s2	0.901	0.199	−0.124
H2s3	0.827	0.255	−0.077
H3	0.204	0.166	−0.357
H3s1	−0.026	0.233	0.332
H3s2	0.013	0.248	0.227
H3s3	−0.138	0.209	0.252
H4	0.110	0.084	−0.418
H4s1	0.016	0.145	0.414
H4s2	−0.088	0.104	0.349
H4s3	0.090	0.086	0.379
H5	0.216	−0.011	−0.331
H6	0.230	0.005	−0.197
H8	0.333	0.015	−0.034
H10	0.311	−0.020	0.109
H13	0.398	0.016	0.413
H14	0.361	−0.060	0.525
H15	0.301	−0.166	0.450
H16	0.247	−0.165	0.299
H17	0.322	−0.099	0.206

Results and Discussion

Complex Preparation. The Mo(VI) diketone complex, $MoO_2(acac)_2$, was used as the source of molybdenum. For a ratio of ligand-to-metal complex of either 2:1 or 1:1, the same brown complex formed as a precipitate. The elemental analysis of the brown complex indicates two metal atoms per ligand as well as the incorporation of one molecule of solvent per molecule of complex, suggesting that one Mo(VI) ion is five-coordinated while

---

(14) (a) Casellato, U.; Tamburini, S.; Vigato, P. A.; de Stefani, A.; Vidali, M.; Fenton, D. E. *Inorg. Chim. Acta* **1983**, *69*, 45. (b) Fenton, D. E.; Gayda, S. E.; Castellato, U.; Vidali, M.; Vigato, P. A. *Inorg. Chim. Acta* **1977**, *21*, L29. (c) Lintvedt, R. L.; Ahmad, N. *Inorg. Chem.* **1982**, *21*, 2356.

(15) Miles, M. L.; Harris, T. M.; Hauser, C. R. *J. Org. Chem.* **1965**, *30*, 1007.

(16) Grace, J.; Chen, J.; McDonald, J. W.; Newton, W. E. *Inorg. Chem.* **1976**, *15*, 11.

(17) O'Connor, C. J.; Sinn, E.; Cukauskas, E. J.; Deaver, B. S., Jr. *Inorg. Chim. Acta* **1979**, *32*, 39.

(18) O'Connor, C. J.; Deaver, B. S., Jr.; Sinn, E. *J. Chem. Phys.* **1979**, *70*, 5161.

(19) Freyberg, D. P.; Mockler, G. M.; Sinn, E. *J. Chem. Soc., Dalton Trans.* **1976**, 447.

(20) Corfield, P. W. P.; Doedens, R. J.; Ibers, J. A. *Inorg. Chem.* **1967**, *6*, 197.

(21) Supplementary material.

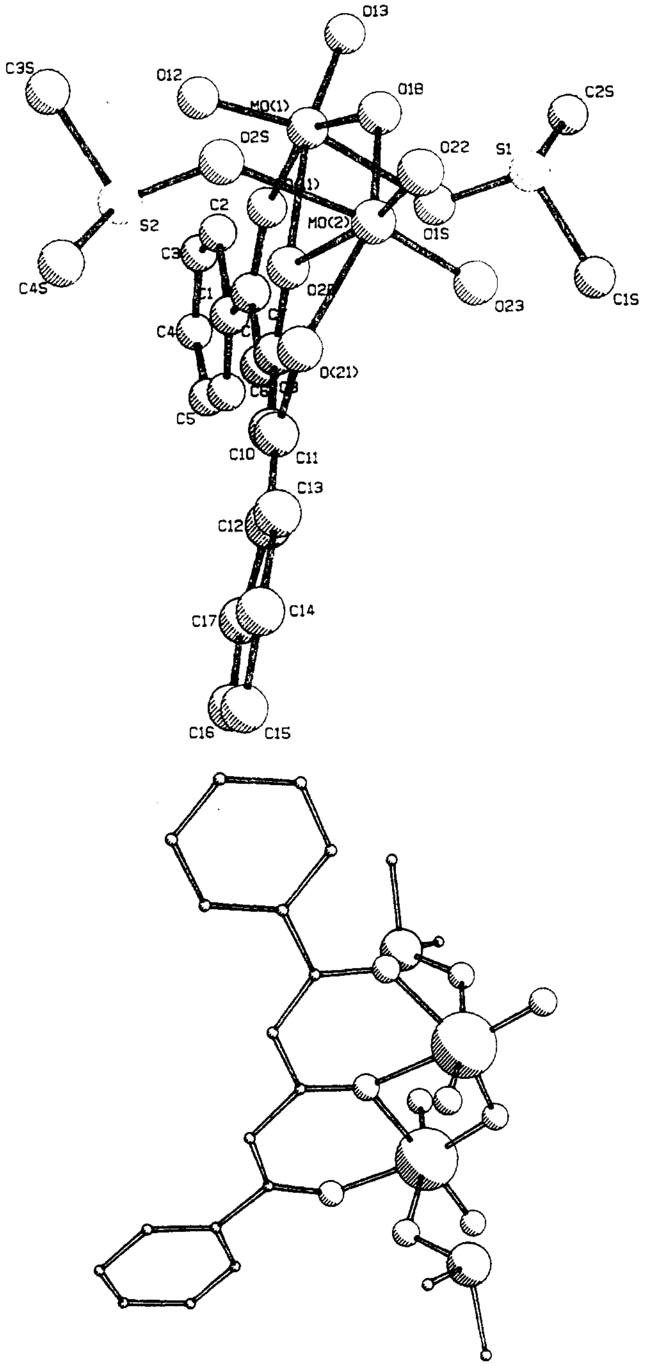

Figure 1. Two views of the binuclear Mo(VI) complex, $(MoO_2)_2(C_{17}H_{12}O_3)(O)(DMSO)_2$.

the other is six-coordinated with an adducted solvent molecule. The complex is extremely insoluble in common organic solvents, but when it is heated vigorously in DMSO, the ethanol molecule is lost and the yellow DMSO adduct is formed. This gradually forms yellow crystals on standing at room temperature.

Structure of the Complex. The structure of the Mo(VI) complex containing two molecules of DMSO was determined by single-crystal X-ray crystallography (Figure 1). The positional coordinates are listed in Table II. The complex is binuclear with a Mo–Mo separation of 3.272 Å. Each of the two molybdenum atoms is in a O_6 environment, forming a distorted octahedron containing *cis*-MoO_2 units. The metal atoms are bridged via an exogenous oxygen atom and endogenous triketonate oxygen. While no crystallographic symmetry governs the internal geometry of the molecule, the halves of the molecule are related by a pseudo-2-fold axis along the bridging oxygens. The two coordinated DMSO molecules are bonded on opposite sides of the principal ligand planes. Selected bond angles and distances are given in Tables III and IV respectively.

Table III. Intramolecular Distances (Å) for $(MoO_2)_2O(PhTriket)(DMSO)_2$

Bond Distances			
Mo1–O12	1.687 (8)	Mo2–O21	2.011 (7)
Mo1–O13	1.698 (8)	Mo2–O2s	2.220 (8)
Mo1–O1b	1.893 (7)	Mo2–O2b	2.240 (7)
Mo1–O11	2.011 (7)	S1–O1s	1.521 (8)
Mo1–O2b	2.215 (7)	S2–O2s	1.528 (8)
Mo1–O1s	2.263 (8)	O2b–C9	1.30 (1)
Mo2–O22	1.682 (7)	O11–C7	1.31 (1)
Mo2–O23	1.705 (8)	O21–C11	1.32 (1)
Mo2–O1b	1.921 (7)		

Nearest Intermolecular Contacts

contact	distance	symmetry operation
O13–C4s	3.23 (1)	$^1/_2 + x, ^1/_2 - y, z - ^1/_2$
O13–C3s	3.27 (1)	$^1/_2 + x, ^1/_2 - y, z - ^1/_2$
O22–C2s	3.29 (2)	$x - ^1/_2, ^1/_2 - y, ^1/_2 + z$

Table IV. Intramolecular Bond Angles (deg)

O12–Mo1–O13	103.2 (4)	O22–Mo2–O21	102.2 (3)
O12–Mo1–O1b	101.3 (3)	O22–Mo2–O2s	87.3 (3)
O12–Mo1–O11	93.1 (3)	O22–Mo2–O2b	167.3 (3)
O12–Mo1–O2b	89.9 (3)	O23–Mo2–O1b	99.4 (3)
O12–Mo1–O1s	164.8 (3)	O23–Mo2–O21	93.4 (3)
O13–Mo1–O1b	101.0 (3)	O23–Mo2–O2s	169.0 (3)
O13–Mo1–O11	101.0 (3)	O23–Mo2–O2b	90.5 (3)
O13–Mo1–O2b	166.9 (3)	O1b–Mo2–O21	148.2 (3)
O13–Mo1–O1s	89.1 (4)	O1b–Mo2–O2s	83.6 (3)
O1b–Mo1–O11	150.1 (3)	O1b–Mo2–O2b	73.1 (3)
O1b–Mo1–O2b	74.2 (3)	O21–Mo2–O2s	79.0 (3)
O1b–Mo1–O1s	84.9 (3)	O21–Mo2–O2b	77.9 (3)
O11–Mo1–O2b	79.8 (3)	O2s–Mo2–O2b	80.2 (3)
O11–Mo1–O1s	75.6 (3)	Mo1–O1b–Mo2	118.2 (3)
O2b–Mo1–O1s	78.4 (3)	C9–O2b–Mo1	131.9 (6)
O22–Mo2–O23	102.2 (4)	C9–O2b–Mo2	127.1 (6)
O22–Mo2–O1b	103.3 (3)	Mo1–O2b–Mo2	94.5 (3)

Table V. Distances and Angles in the Coordination Spheres of 1,3,5-Triketonates

	interatomic distances, Å		
complex	M_1–M_2	M–O_t	M–O_{b2}
$Co_2(DBA)_2(py)_2$	3.27	2.01	2.09
$Ni_2(DBA)_2(py)_2$	3.17	2.01	2.04
$Cu_2(BAA)_2(py)_2$	3.05	1.91	1.95
$Mo_2O_4(DBA)(O)(DMSO)_2$	3.274 (3)	2.011 (7) 2.011 (7)	2.240 (7) 2.215 (7)

	interatomic angles, deg		
complex	O_{b1}–M–O_{b2}	M–O_{b2}–M	M–O_{b1}–M
$Co_2(DBA)_2(py)_2$	77.3	102.7	
$Ni_2(DBA)_2(py)_2$	78.5	101.5	
$Cu_2(BAA)_2(py)_2$	76.6	103.4	
$Mo_2O_4(DBA)(O)(DMSO)_2$	74.2 (1) 73.1 (2)	94.5 (2)	118.2 (2)

The ligand remains essentially flat. It is near to coplanar with the central Mo_2O_2 bridging unit. The angle between these two planes is 14.5°. The two metal atoms differ significantly in geometry, but both are considered to be pseudooctahedral Mo(VI) ions, on the basis of the arguments presented below. The O=Mo=O angles of 103.2 (4) and 102.2 (4)° are in the normal range for those compounds containing cis units.[22,23] The most significant difference between the Mo complex structure and that of the other structures studied is the bridging angle between the two metal atoms and the ligand. This angle is considerably smaller in the Mo(VI) complex due to the larger atomic size of the metal atom. Bond distances are comparable.

---

(22) Butcher, R. J.; Penfold, B. R.; Sinn, E. *J. Chem. Soc., Dalton Trans.* **1979**, 668.

(23) Sorrell, T. N.; Ellis, D. J.; Cheesman, E. H. *Inorg. Chim. Acta* **1986**, *113*, 1.

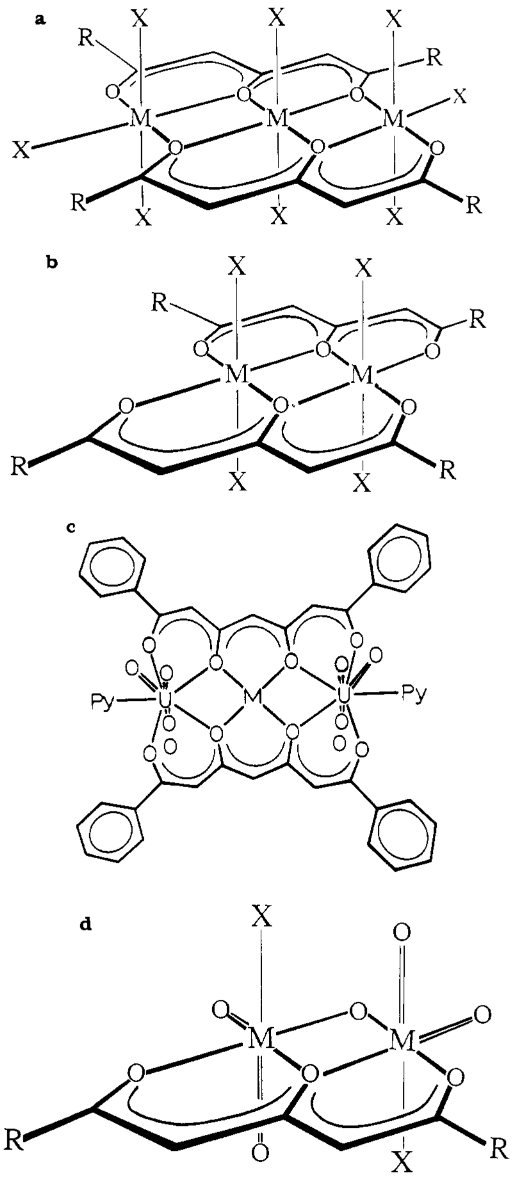

Figure 2. Generalized structures for polyketonate complexes together with the structure of $(MoO_2)_2(C_{17}H_{12}O_3)(O)(DMSO)_2$. (a) M = Ni, Cr; X = Cl^-, OH^-; R = CH_3, C_6H_5. (b) M = Cu, Ni, Co, VO, Fe; X = Cl^-, OH^-; R = CH_3, C_6H_5. (c) M = Mn, Fe, Co, Ni. (d) Present complex: M = Mo; X = DMSO; R = C_6H_5.

Generalized structures for triketone complexes, along with the structure for the Mo(VI) complex, are shown in Figure 2. The requirement of cis oxygen atoms in the MoO_2 unit limits the structural capabilities and a 1:1 metal-to-ligand complex does not form as with other metal atoms. A comparison of interatomic distances and interatomic angles for some of the β-polyketone complexes is given in Table V. The nomenclature for Table V is based on **1**. The angles in the Mo_2O_2 bridging center generally show greater deviation from 90° than do the centers in the analogous first row complexes. This is presumably due to the rigid geometrical requirements of the dioxomolybdenum(VI) unit and the asymmetry of the ligand environment in having a triketone on one side of the plane and an $-O^{2-}-$ bridge on the other. The bond to the ketonic bridging oxygen is longer than in the first-row complexes, presumably due to the short $Mo-O^{2-}$ bond (1.907 Å).

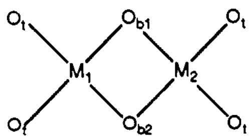

1

Magnetic Properties. The complex was prepared from Mo(VI) starting materials, and in the absence of evidence of significant redox reactions, a presumption of Mo(VI) in the product is reasonable. This configuration has no d electrons, so there is no strong drive from the metal in favor of any particular geometry. The preferred geometry should therefore be governed by the steric and electrostatic predisposition of the ligand. The Mo(V) oxidation state is also stable for this metal and is frequently observed. This could arise if two of the MoO_2 oxygens were protonated, or if one of these and the exogenous oxygens were protonated. In this state, the d^1 configuration adds a crystal field stabilization that favors regular octahedral geometry. The presence of spin–orbit coupling in octahedral d^1 to lift the degeneracy eliminates the need for Jahn–Teller splitting in this system.

To examine the possibility of Mo(V) species in the structure, the magnetic properties were closely examined. Over the entire temperature range, the molecule shows a very low level of paramagnetism, with the effective Bohr magneton number μ_{eff} rising from 0.18 μ_B at 35 K to 0.40 μ_B BM at 277.1 K (detailed temperature dependence given in the supplementary material). The latter value corresponds to about 5.4% of an unpaired electron. This indicates a small proportion of paramagnetic impurity, possibly small amounts of Mo(V). The small magnitude of the remainder of the magnetic susceptibility could be explained most readily in terms of the diamagnetic Mo(VI) configuration. The low magnetism could also be explained by very strong antiferromagnetic coupling between a pair of oxygen-bridged Mo(V) species, but the temperature-independent paramagnetism (constant χ) expected for such a system is lacking.

Spectroscopic Measurements. The diketone complex $MoO_2(acac)_2$ exhibits one peak at 280 nm (log ϵ = 3.97) in the UV region. The triketone complex exhibits three peaks: 280 (log ϵ = 4.03), 405 (log ϵ = 3.99), and 446 nm (log ϵ = 4.10). Because of the high extinction coefficients, these peaks are assigned to ligand-to-metal charge-transfer transitions. The peak positions are at lower energies than those observed in diketone complexes. This is compatible with lowering of the charge-transfer energy by to the greater conjugation in the triketone system compared with the diketones.[6,24] There is no evidence of d–d transitions, in keeping with a Mo(VI) configuration.

The strong peaks at 960 and 970 cm^{-1} in the IR region are assigned to the stretching mode of *cis*-MoO_2 units.[25] The strong peaks at 820 and 850 cm^{-1} are assigned to the bridging oxygens.[23,26,27]

All hydrogen atoms are accounted for in the NMR spectra, and the chemical shifts (downfield from tetramethylsilane) in DMSO-d_6 solution are 7.85 (phenyl *p*-H), 7.59 (phenyl *o,m*-H), 7.52 (H on ligand), and 2.08 ppm (CH_3 on DMSO). The shifts are comparable to those reported for similar compounds.[25]

Electrochemistry. The $(MoO_2)_2$ triketonate complex undergoes irreversible reductions at ∼−0.9 and ∼−1.1 V in DMSO solution vs SSCE, while the diketone–MoO_2 complex shows an irreversible reduction at −1.2 V. Since these reductions are irreversible, the electrochemical data are for E_{pc}, which is the potential measured at the maximum cathodic peak current. These data indicate a one-step reduction, for the diketonate, to the Mo(V)–oxo species. It is most probable that the analogous reduction of the triketonate to the corresponding Mo(V)–oxo species proceeds in two one-electron steps, one for each of the two Mo(VI) sites. The more facile reduction of the metals in $(MoO_2)_2(C_{17}H_{12}O_3)(O)(DMSO)_2$ is consistent with the more extensive π-electron system of the triketone ligand over that of acac. The ability of the oxo-bridged and adducted solvent to act as a weak electron-withdrawing group could enhance this effect. Studies by Topich et al.[28] and Naka-

---

[24] Dunn, T. In *Modern Coordination Chemistry*; Lewis, J.; Wilkinson, R. G., Eds.; Interscience: New York, 1960.

[25] Mitchel, P. C. H. *Q. Rev., Chem. Soc.* **1966**, *20*, 103.

[26] Melby, R. L. *Inorg. Chem.* **1969**, *8*, 343.

[27] Hill, A. G.; Atabay, N.; McAuliffe, C. A.; McCullough, F. P.; Razzoki, S. M. *Inorg. Chim. Acta* **1979**, *35*, 35.

[28] Topich, J. *Inorg. Chim. Acta* **1980**, *46*, L37. Topich, J.; Lyon, III, J. T. *Inorg. Chem.* **1984**, *23*, 3202.

mura et al.[29] support this: delocalization or withdrawal of electrons from the metal center makes it easier for a complex to accept additional electrons. For example, the Mo(VI) to Mo(V) reduction potential for the S-ligated, delocalized $MoO_2(Et_2dtc)_2$ is −0.83 V (Me_2SO)[30] while in the less delocalized O-ligated $MoO_2(ox)_2$ it is −1.07 V (Me_2SO).[31]

As might be expected, the complex is like a binuclear version of the diketonate $MoO_2(acac)_2$, which functions as an olefin epoxidation and an ethanol oxidation catalyst.[11-13] The catalytic properties of the triketonate complexes are under investigation to see if the binuclearity confers any advantage.

Acknowledgment. Support from NSF Grants CHE-8300516 and CHE-8609272 and a Faculty Research Grant from CSUS are gratefully acknowledged.

Supplementary Material Available: Tables listing magnetic moments, thermal parameters, bond lengths and angles associated with non-hydrogen atoms, and least-squares planes and a figure depicting a cyclic voltammogram (13 pages); a table of calculated and observed structure factors (16 pages). Ordering information is given on any current masthead page.

---

(29) Nakamura, A.; Nakayama, M.; Subihashi, K.; Otsuka, S. *Inorg. Chem.* **1979**, *18*, 394.

(30) DeHayes, L. J.; Faulkner, H. C.; Doub, W. H., Jr.; Sawyer, D. T. *Inorg. Chem.* **1975**, *14*, 2110.

(31) Isbell, A. F.; Sawyer, D. T. *Inorg. Chem.* **1971**, *10*, 2449.

Contribution from the Institute of Inorganic Chemistry,
University of Zürich, Winterthurerstrasse 190, 8057 Zürich, Switzerland

Synthesis and Structure of Dimeric Metal Complexes with N(3)/N(9)-Chelating Hypoxanthine Ligands and with Bridging Water Molecules: $[M_2(\mu\text{-hyxan})_2(SO_4)_2(\mu\text{-}H_2O)_2(H_2O)_2]$ (M = Cu, Cd, Zn; hyxan = Hypoxanthine)

Erich Dubler,* Gaby Hänggi, and Helmut Schmalle

Received August 4, 1989

Three new dimeric metal complexes of hypoxanthine (hyxan) with the general formula $M^{II}(hyxan)SO_4\cdot 2H_2O$ with M = Cu, Zn, or Cd have been synthesized from acidic aqueous solutions. They all crystallize in the triclinic space group $P\bar{1}$ with two formula units per cell. The cell dimensions are a = 7.470 (2) Å, b = 8.529 (2) Å, c = 8.675 (2) Å, α = 77.32 (2)°, β = 87.70 (2)°, γ = 65.40 (2)°, and V = 489.5 (7) Å^3 for $Cu(hyxan)SO_4\cdot 2H_2O$, a = 7.278 (2) Å, b = 8.714 (4) Å, c = 8.789 (8) Å, α = 102.45 (5)°, β = 91.46 (4)°, γ = 113.05 (3)°, and V = 497.1 (3) Å^3 for $Zn(hyxan)SO_4\cdot 2H_2O$, and a = 7.343 (1) Å, b = 8.856 (1) Å, c = 9.002 (3) Å, α = 101.55 (2)°, β = 92.36 (3)°, γ = 112.86 (1)°, and V = 523.9 (4) Å^3 for $Cd(hyxan)SO_4\cdot 2H_2O$. The structures of the copper and cadmium complexes were refined on the basis of 2809 and 6857 observed reflections to R values of 0.055 and 0.036, respectively. Single-crystal and powder X-ray data indicate that the zinc complex is virtually isostructural with its cadmium and copper analogues. The complexes exhibit a new dimeric structure type with molecular centrosymmetric units, $[M_2(\mu\text{-hyxan})_2(SO_4)_2(\mu\text{-}H_2O)_2(H_2O)_2]$. The two metal atoms are bridged by two N(3)/N(9)-chelating hypoxanthine ligands and by two water molecules. The metal–metal distances are 3.151 (1) Å (Cu) and 3.452 (1) Å (Cd). Distorted octahedral coordination of the metal atoms by two N and by four O atoms is observed with a pronounced (4 + 1 + 1) elongation of the octahedron in the copper complex. The bridging water molecules are stabilized by very strong hydrogen bonds of the type O–H⋯O with a minimum O⋯O distance of 2.57 Å. In the neutral hypoxanthine ligand, hydrogen atoms are attached at N(1) and N(7), which are involved in hydrogen bonds of the type N–H⋯O(sulfate). The purine rings are stacked, rotated 180° with respect to each other, with stacking distances of 3.34 and 3.30 Å, respectively. A review of X-ray structure determinations of metal–hypoxanthine complexes as well as of polynuclear copper and cadmium complexes with bridging water molecules is given.

Introduction

The stereochemistry of complexes formed between metal ions and nucleic acid bases, nucleosides, or nucleotides is believed to be important in determining the activity of many compounds of biological interest.[1,2]

The coordination properties of adenine and guanine, the major purine bases present in DNA and RNA, have been the subject of different crystallographic studies.[3,4] In contrast, only a few structures of metal complexes of the oxopurines hypoxanthine (hyxan), xanthine, uric acid, or allopurinol are available.

Hypoxanthine (1,7-dihydro-6*H*-purin-6-one) occasionally occurs as a constituent of the nucleoside inosine in minor amounts in transfer RNA.[5] It also is an intermediate product of purine metabolism, formed by enzymatical degradation of nucleic acids. The molybdenum- and iron-containing enzyme xanthine oxidase catalyzes the biological oxidation of hypoxanthine via xanthine to uric acid, which subsequently is released from the active site of the enzyme.[6] Defects in purine metabolism result in an increase of the uric acid level and in the deposition of sodium hydrogen urate monohydrate crystals in joints. This disease, known as gout, is clinically treated by the drug allopurinol (pyrazolo[3,4-*d*]pyrimidin-6-one), which also is a substrate for xanthine oxidase.[7] Alloxanthine (pyrazolo[3,4-*d*]pyrimidin-2,6-dione), the enzymatic oxidation product of allopurinol, is believed to remain bound to the reduced form of the molybdenum center of xanthine oxidase, thus inactivating the enzyme and inhibiting uric acid formation.[8]

Previous crystallographic investigations of metal complexes of unsubstituted hypoxanthine have elucidated three different coordination types. They are labeled I, IIb, and III in the coordination scheme given in Figure 1.

Type I represents monomeric complexes with monodentate coordination of hypoxanthine through the nitrogen atom N(7). In dimeric complexes of *type IIb*, two metal ions are bridged by four N(3)- and N(9)-chelating hypoxanthine ligands. *Type III* finally involves a polymeric complex, where hypoxanthine is coordinating through N(3) and N(7) to different metal ions, forming

---

* To whom correspondence should be addressed.

(1) Barton, J. K.; Lippard, S. J. In *Nucleic Acid Metal Interactions*; Spiro, T. G., Ed.; Metal Ions in Biology, Vol. 1; Wiley: New York, 1980; p 31.

(2) Marzilli, L. G.; Kistenmacher, T. G.; Eichhorn, G. L. In *Nucleic Acid-Metal Interactions*; Spiro, T. G., Ed.; Metal Ions in Biology, Vol. 1; Wiley: New York, 1980; p 179.

(3) Hodgson, D. J. *Prog. Inorg. Chem.* **1977**, *23*, 211.

(4) Sletten, E. G. *The Jerusalem Symposia on Quantum Chemistry and Biochemistry*; Jerusalem Academy of Sciences and Humanities: Jerusalem, 1977; Vol. 9, p 53.

(5) Hurst, D. T. In *An Introduction to the Chemistry and Biochemistry of Pyrimidines, Purines and Pteridines*; Wiley: New York, 1980; p 179.

(6) Stiefel, E. J. *Prog. Inorg. Chem.* **1977**, *22*, 1.

(7) Hille, R.; Massey, V. In *Nucleic Acid Metal Interactions*; Spiro, T. G., Ed.; Metals Ions in Biology, Vol. 7; Wiley: New York, 1985; p 443.

(8) Hawkes, T. R.; George G. N.; Bray, R. C. *Biochem. J.* **1984**, *218*, 961.

0020-1669/90/1329-2518$02.50/0 © 1990 American Chemical Society